

## N O T I C E

THIS DOCUMENT HAS BEEN REPRODUCED FROM  
MICROFICHE. ALTHOUGH IT IS RECOGNIZED THAT  
CERTAIN PORTIONS ARE ILLEGIBLE, IT IS BEING RELEASED  
IN THE INTEREST OF MAKING AVAILABLE AS MUCH  
INFORMATION AS POSSIBLE

(NASA-CR-152361) JET-DIFFUSER EJECTOR -  
ATTACHED NOZZLE DESIGN Final Report (Flight  
Dynamics Research Corp.) 41 p HC A03/MF A01  
CSCS 200

N81-19412

Unclas  
G3/34 17797

## JET-DIFFUSER EJECTOR - ATTACHED NOZZLE DESIGN

by

Morton Alperin and Jiunn-Jeng Wu

May 1980

Distribution of this report is provided in the interest of information  
exchange. Responsibility for the contents resides  
in the authors or organization that prepared it.

Prepared under Contract No. NAS2-10059 by  
FLIGHT DYNAMICS RESEARCH CORPORATION  
Van Nuys, Ca.

for

AMES RESEARCH CENTER  
NATIONAL AERONAUTICS AND SPACE ADMINISTRATION

and

NAVAL AIR DEVELOPMENT CENTER  
WARMINSTER, PENNSYLVANIA



# JET-DIFFUSER EJECTOR - ATTACHED NOZZLE DESIGN

by

Morton Alperin and Jiunn-Jenq Wu

May 1980

Distribution of this report is provided in the interest of information exchange. Responsibility for the contents resides in the authors or organization that prepared it.

Prepared under Contract No. NAS2-10059 by  
FLIGHT DYNAMICS RESEARCH CORPORATION  
Van Nuys, Ca.

for

AMES RESEARCH CENTER  
NATIONAL AERONAUTICS AND SPACE ADMINISTRATION

and

NAVAL AIR DEVELOPMENT CENTER  
WARMINSTER, PENNSYLVANIA

### Abstract

The original design of the jet-diffuser ejector included the use of detached nozzles, to permit injection of primary fluid upstream of the inlet to the ejector. This design proved objectionable from the point of view of integration into high speed aircraft configurations. Problems of stowage and duct design imposed a requirement for design of primary nozzles which could be stowed during conventional flight with a minimum of complexity and drag.

The development of attached primary nozzles to replace the detached nozzles originally used on the jet-diffuser ejector is described in detail. Problems associated with the internal flow efficiency and the influence of nozzle fairing design on external flow are discussed. The final design is utilized for an investigation of the sensitivity of the ejector to surface irregularities which might occur in ejector installation and operation.



### Nomenclature

$A_2$	cross-section area of ejector throat
$a_\infty$	primary jet area when actual mass flow is expanded isentropically to ambient pressure
$C$	discharge coefficient
$F$	net thrust
$\dot{m}$	mass flow
$n$	$(\gamma - 1)/\gamma$
$V$	Velocity
$p, P$	absolute pressure
$R$	gas constant
$s_\infty$	diffuser jet area when actual mass flow is expanded isentropically to ambient pressure
$x, y, z$	coordinates
$X_2$	throat width of ejector
$\alpha_\infty$	$= (A_2/a_\infty)$ , inlet area ratio
$\Gamma$	circulation
$\gamma$	ratio of specific heats
$\psi$	stream function
$\eta_N$	nozzle thrust efficiency
$\theta$	angle of primary injection with respect to normal to plane of symmetry
$\phi$	thrust augmentation = ejector net thrust/isentropic reference jet net thrust
$\phi'$	thrust augmentation for tubular nozzles
$\omega$	induced flow angle, defined similar to $\theta$

### Subscripts

$o$	stagnation
$p$	primary jet
$\infty$	ambient condition

### List of Figures

<u>Figure No.</u>	<u>Title</u>	<u>Page</u>
1	Alperin Jet-Diffuser Ejector Model 0232	4
2	FDRC Static Ejector Test Rig	5
3	Segmented Slot Coanda Nozzle, Geometry and Performance	7
4	Adjustable, Tubular Nozzles, Adjacent to Inlet Surface, Geometry and Performance	9
5	Primary Nozzle #1, $\theta = 55^\circ$ (Constant $\phi'$ map)	10
6	Primary Nozzle #1, $\theta = 60^\circ$ (Constant $\phi'$ map)	11
7	Primary Nozzle #1, $\theta = 65^\circ$ (Constant $\phi'$ map)	12
8	Primary Nozzle #2 $\theta = 55^\circ$ (Constant $\phi'$ map)	13
9	Primary Nozzle #3 $\theta = 50^\circ$ (Constant $\phi'$ map)	14
10	Primary Nozzle #3 $\theta = 55^\circ$ (Constant $\phi'$ map)	15
11	Primary Nozzle #3 $\theta = 60^\circ$ (Constant $\phi'$ map)	16
12	Potential Flow Model of Ejector Inlet	17
13	Performance of Jet-Diffuser Ejector With Adjustable Nozzles, Compared to Performance with Detached Nozzles	19
14	Attached Primary Nozzles No. 4 and 4A, Mounted on Jet-Diffuser Ejector	21
15	Primary Nozzle No. 5 on AJDE	23
16	Jet-Diffuser Ejector - Cross-Section with Surface Irregularities	27

List of Tables

<u>Table No.</u>	<u>Title</u>	<u>Page</u>
I	Adjustable Primary Nozzles	18
II	Attached Nozzle Properties	22
III	Nozzle Performance	24
IV	Surface Irregularities	26
V	Dimensions of Surface Protrusions	28
VI	Influence of Throat Protrusions at Center of Span	30

## Table of Contents

Introduction	1
Test Apparatus	2
Experimental Uncertainties	2
Mass Flow	2
Static Pressure	3
Forces	3
Test Results	6
Segmented Primary Nozzles	6
Adjustable Tubular Primary Nozzles	8
Attached Nozzles	20
Primary Nozzle Performance	24
Discharge Coefficient	24
Thrust Efficiency	24
Sensitivity Study	26
Inlet Surface Irregularities	28
Protrusions	28
Corners	28
Center of Span	28
Plenum Leakage	29
Corner	29
Center of Span	29
Depression	29
Corner	29
Asymmetry	30
Throat Irregularities	30
Protrusions	30
Corner	30
Center of Span	30
Plenum Leakage	31
Corner	31
Center of Span	31
Diffuser Irregularities	31
Protrusions	31
Corner	31
Center of Span	31
Conclusions	32
References	33

## Summary

The development of attached primary nozzles to replace the detached nozzles of the original jet-diffuser ejector has been described in detail. Initially, slotted primary nozzles located at the inlet lip and injecting fluid normal to the thrust axis, and rotating the fluid into the thrust direction using the Coanda Effect was investigated. Experiments indicated excessive skin friction or momentum cancellation due to impingement of opposing jets resulted in performance degradation. This indicated a desirability for location and orientation of the injection point at positions removed from the immediate vicinity of the inlet surface, and at an acute angle with respect to the thrust axis.

To estimate the ideal injection point location and orientation, three sets of adjustable, tubular nozzles with differing spacing and tube size, were tested over a range of positions and orientations. The results were summarized in a series of maps of constant augmentation lines drawn on the inlet area of the ejector. From this study and consideration of the problems of aircraft integration of the ejector, and internal and external nozzle losses, a geometry for the attached nozzles was selected.

The first set of primary, attached nozzles exhibited high internal efficiency, but the external configuration resulted in flow separation and unsteady flow through the ejector. The lengthening of the external fairing chord alleviated the instability but the large blockage loss and remaining sensitivity to inlet disturbances indicated a requirement for a reduction of the thickness and thickness ratio of the primary nozzles.

A third set of attached primary nozzles was designed to reduce the thickness of the nozzle fairing and therefore the blockage of the induced flow. To accomplish this it was necessary to elongate the internal duct shape and to reduce the wall thickness of the nozzles. These modifications of the design resulted in an increase of the turning loss of the primary jet, but the instability and sensitivity to inlet disturbances was virtually eliminated.

A sensitivity study, aimed at the determination of the effect of leaks, protrusions, depressions and asymmetries in the ejector surfaces was then carried out. The results indicated a relative insensitivity to all surface irregularities, except for large protrusions at the throat of the ejector.

## INTRODUCTION

The jet-diffuser ejector was originally developed for application as a propulsive, lifting, controlling element of the Small Tactical Aerial Mobility Platform (STAMP) vehicle. Its characteristics and performance are described in Reference 1. Although that configuration was suitable for its intended low speed use, integration into a high speed aircraft required further development.

The STAMP Ejector as originally designed had a rectangular cross-section with flat non-diverging ends. To avoid collapse of the flow pattern after discharge from the diffuser, the flat ends were extended beyond the sides of the diffuser with a semi-circular end plate. This feature, although acceptable for the STAMP vehicle application, presented an undesirable source of complexity when integrated into a high speed aircraft design. To eliminate the requirement for these end plates, a three-dimensional diffuser was developed for the jet-diffuser ejector. The development of this three-dimensional design is described in Reference 2 and the resulting ejector configuration is illustrated on Figure 1.

The original design of the STAMP ejector also had protruding, detached primary nozzles which were utilized for the purpose of achieving sufficient mixing of injected and induced flows in the short, jet-diffuser ejector. However, the application of this ejector for use in V/STOL maneuvering of a high speed aircraft imposed the requirement for stowage of these nozzles during the high speed portion of the flight spectrum to avoid excessive drag. In addition, the separation of the nozzles from the body of the ejector imposed a requirement for excessively complex ducting arrangements. Thus, an attempt was made to design attached nozzles which could be supplied with energized gas from the duct within the ejector's body, while avoiding excessive internal and external nozzle losses, and maintaining the high performance characteristic of jet-diffuser ejectors.

The development of the attached nozzles, the performance of the ejector with these nozzles, and the influence of surface irregularities and leaks upon the performance are discussed in this document.

## TEST APPARATUS

The rectangular jet-diffuser ejector previously utilized for the development of the three-dimensional diffuser (Fig. 1) was used as a basis for testing the various forms of attached nozzle designs. Testing was performed on the FDRC Static Test Rig where measurements of forces, mass flow rates, pressures and temperatures were made to permit evaluation of the ejector performance.

The FDRC Static Test Rig is shown on Figure 2. The test rig structure consists of two basic components; a fixed frame assembly secured to the foundation, and a rigid assembly consisting of the air supply piping and the ejector, supported by three bearing balls. This latter assembly is thus free to rotate and translate on a horizontal plane, restricted only by two flexible bellows and three load cells which provide force and moment measurements.

Air is supplied by a rotary, positive displacement blower to a large plenum chamber. Distribution of the compressed air and control of its mass flow rate and pressure is accomplished by three remotely controlled valves. One valve each on the primary and diffuser jet supply lines, and a dump valve on the by-pass line. The mass flow rate in each supply line is measured with the aid of calibrated sharp edge orifices and pressure and temperature sensors.

The forces on the ejector are transferred through the floating structure to the load cells whose readings were precisely calibrated to permit evaluation of the tare forces introduced into the system by the flexible bellows and the pressurization of the system.

Pressure, temperature and force measurements by the transducers are transmitted to a digital readout at the control panel.

### Experimental Uncertainties

#### Mass Flow

The techniques described in Reference 3 were used to evaluate the mass flow rates to the primary and diffuser jets. Correlation with standard orifices indicated maximum variation less than 0.5% in the mass flow at the test conditions.

### Static Pressure

Calibration of the static pressure readings on the digital equipment compared to the readings on a calibrated instrument and manometer, indicated an uncertainty of less than 1% of the gage pressure at the test conditions.

### Forces

Under static conditions the force measurements are accurate to 0.5% of the maximum thrust force. Under ejector test conditions the force readings are taken as an average of about 40 readings per run showing a standard deviation of less than 0.5% of the mean thrust.



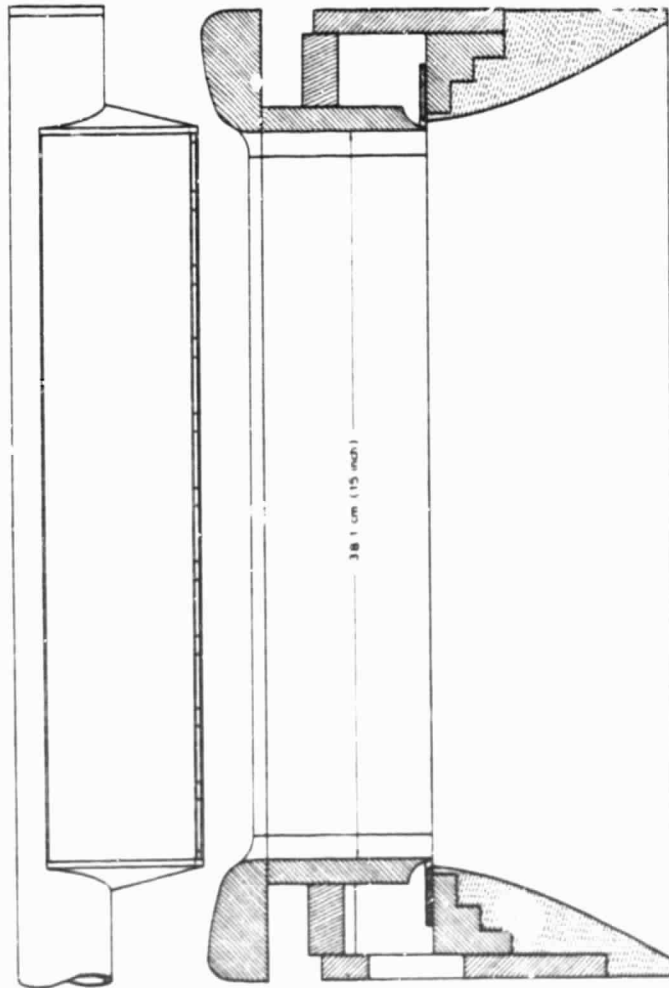
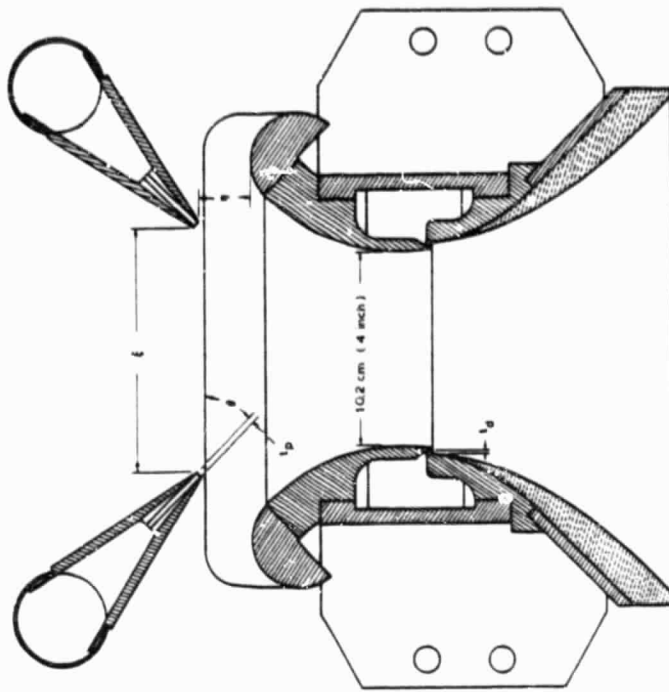
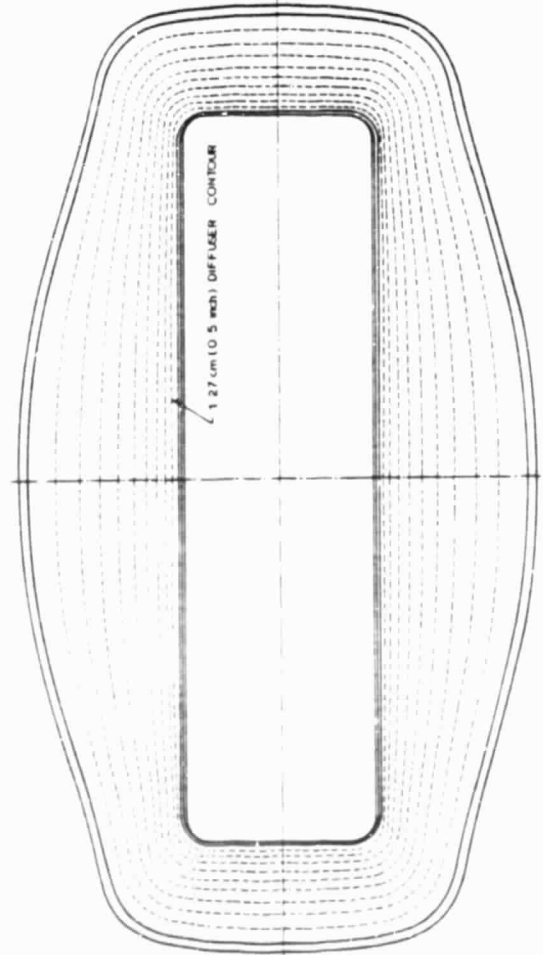


Figure 1  
ALPERIN JET-DIFFUSER EJECTOR

Model 0232

1978



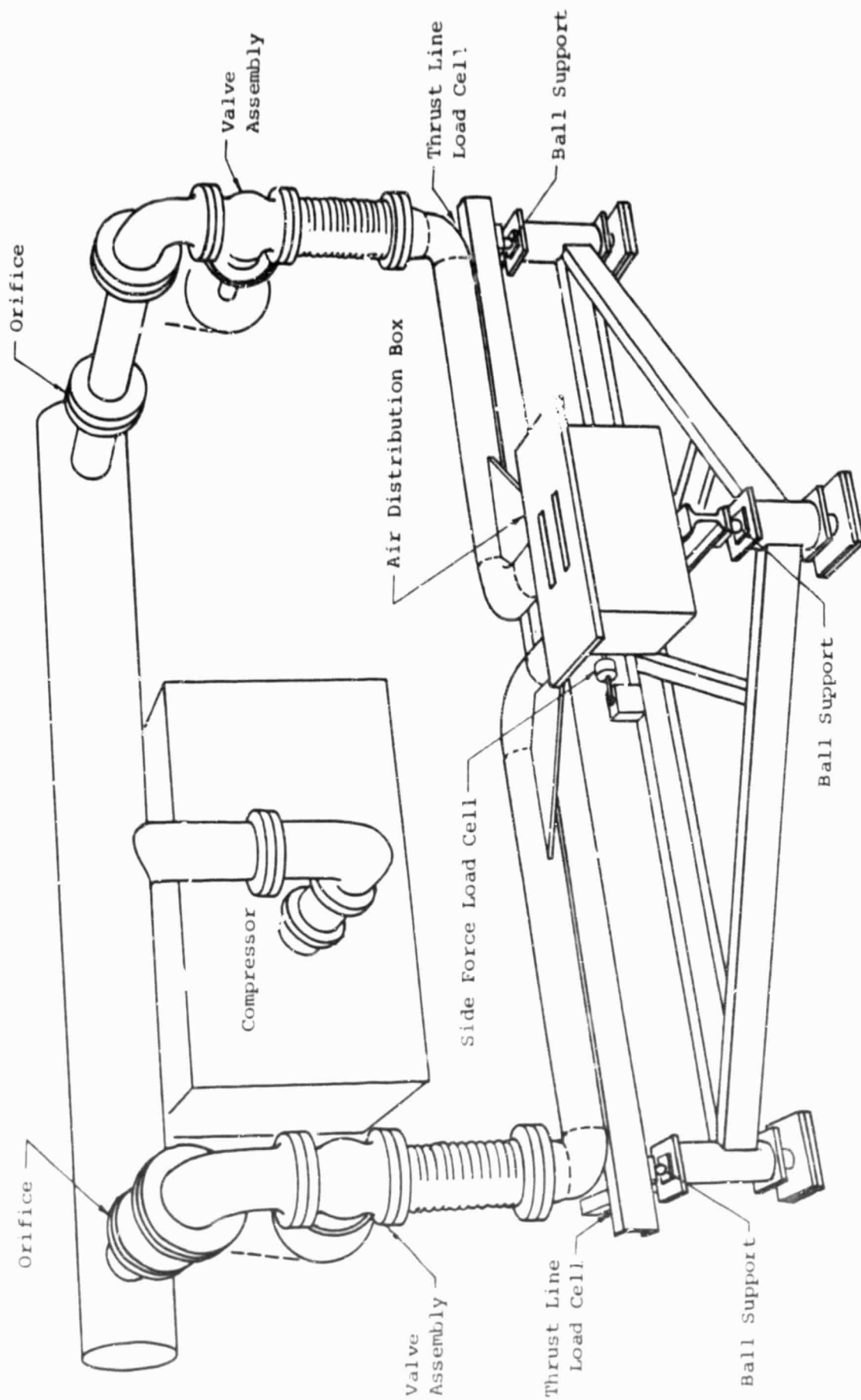


Figure 2. FDRC Static Ejector Test Rig

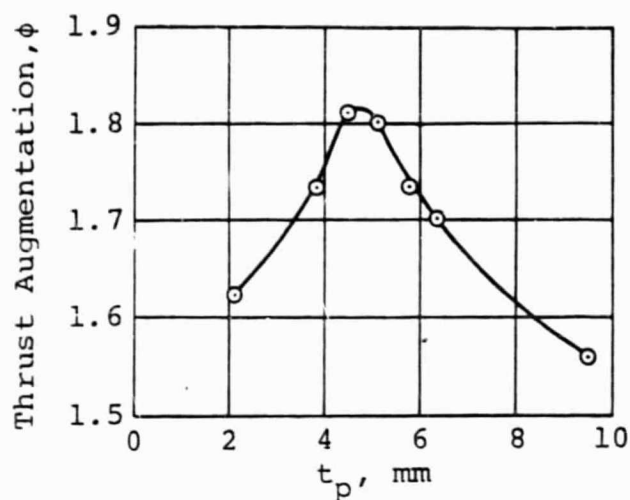
## TEST RESULTS

The detached, protruding, primary nozzles utilized on the STAMP Ejector although suitable for that application, represent an integration difficulty when applied to a high speed aircraft for V/STOL maneuvering. Previous attempts to attach the nozzles to the inlet of the ejector, and to utilize the Coanda Effect to direct the flow towards the thrust direction, resulted in serious penalties in performance, due to the large losses attributable to the skin friction on the inlet surfaces. To reduce these losses, the primary nozzles were segmented as described below and illustrated on Figure 3.

### Segmented Primary Nozzles

The primary slot thickness ( $t_p$ ) was varied over a range from 2.1 mm to 9.5 mm, maintaining a constant individual slot area of  $.605 \text{ cm}^2$ . Since the ejector's throat is 10.2 cm wide and 38.1 cm long, and since there were ten slots per side the ratio of throat area to nozzle area is about 32. With a fixed diffuser jet area and local and viscous flow effects, this corresponds to an area ratio  $A_2/(s_\infty + a_\infty)$  of 21 as determined from measurements of mass flow rates and plenum conditions in both the primary and diffuser jet flows. This arrangement, tested at a plenum pressure of 24.1 kilopascals (gage) (3.5 psig) produced an ejector performance as shown on Figure 3. The thrust augmentation increased to a value of 1.82 as the slot thickness increased from 2.1 mm to about 4.4 mm, and decreased rapidly as the slot thickness was further increased. The rationale for this behavior is as follows:

Since for a fixed diffuser design, thrust augmentation is improved by mixing and is adversely affected by friction, the smaller slot thicknesses create more contact surface between the primary jet and the ejector surface and result in an adverse influence due to skin friction. The rapid turning of these thin jet sheets also prevent effective mixing. As the slot thickness is increased, the skin friction becomes less predominant, the turning less effective and the mixing and performance are improved. Further increase of the slot thickness to values larger than 5.1 mm causes impingement of the flows from opposing primary nozzles upon each other, due to ineffective turning, resulting in momentum cancellation, creating a distorted flowfield which cannot entrain the surrounding fluid effectively, thus resulting in a corresponding decrease in thrust augmentation.



Slot Area =  $0.605 \text{ cm}^2$  each

Pitch = 3.81 cm

Ejector Throat Width = 10.2 cm

Length = 38.1 cm

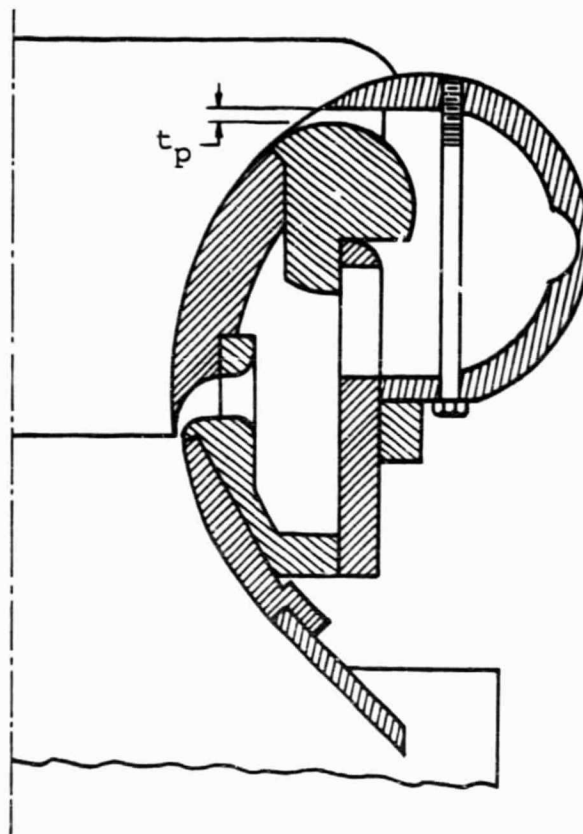


Figure 3 Segmented Slot Coanda Nozzle  
Geometry and Performance

Obviously, these factors indicate a requirement to inject the primary fluid at a position and at an angle which can establish a proper ejector flowfield and avoid momentum cancellation while providing adequate mixing. To determine the optimal injection position and orientation, a study using adjustable primary nozzles was undertaken.

### Adjustable Tubular Primary Nozzles

To examine the influence of the position, orientation and spacing of the primary nozzles, three pairs of primary nozzles which were adjustable in position and orientation were designed, fabricated and tested over a range of positions and orientations. These nozzles were of circular cross-section, 10.2 cm long and attached to a supply duct with an outside diameter of 5.1 cm. The configuration of these three sets of adjustable primary nozzles are described in Table 1 and their appearance, mounted on the ejector is illustrated on Figure 4.

Thrust augmentations reported for these adjustable nozzles ( $\phi'$ ) were evaluated as the ratio of the total force on the ejector measured with load cells, to the thrust of a reference jet. The reference jet is a free jet whose mass flow is equal to that which is injected into the ejector and whose exit velocity is that resulting from an isentropic expansion from the plenum temperature and stagnation pressure measured at the center of a primary nozzle exit to ambient pressure. It is estimated that this reference jet thrust is larger than the actual injected momentum, and therefore the data is conservative. Initially, the No. 1 nozzles were located immediately adjacent to the inlet surface and their angle was varied from  $0^\circ$  to  $45^\circ$ . The set-up and results of this series of tests are shown on Figure 4. As shown the maximum thrust augmentation was achieved at  $45^\circ$ ; an angle which corresponds to the slope of the inlet surface at the nozzle location. Greater inclination of the nozzles will lead to impingement of the primary flow upon the inlet surface with the expected drop in performance.

Tests performed with the nozzles separated from the surface, utilized an extension of 3.81 cm as illustrated on Figures 5 - 11, to provide space and avoid extensive modification of the existing ejector inlet, for the eventual installation of the attached nozzles, as illustrated on Figure 15. The results of these tests were organized and mapped as constant augmentation lines on the ejector inlet area as illustrated on Figures 5 through 11. The particular orientations ( $\theta$ ), utilized for the tests were selected on the basis of practical nozzle design and ejector performance considerations. Additional tests were limited by scheduling considerations. As can be observed on Figures 5 - 11, a distinct optimal point existed for each nozzle inclination.

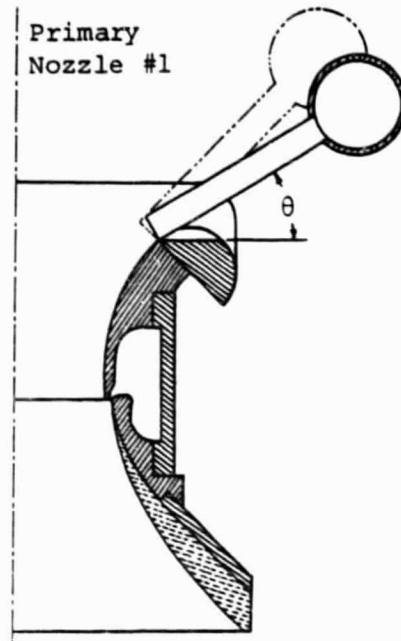
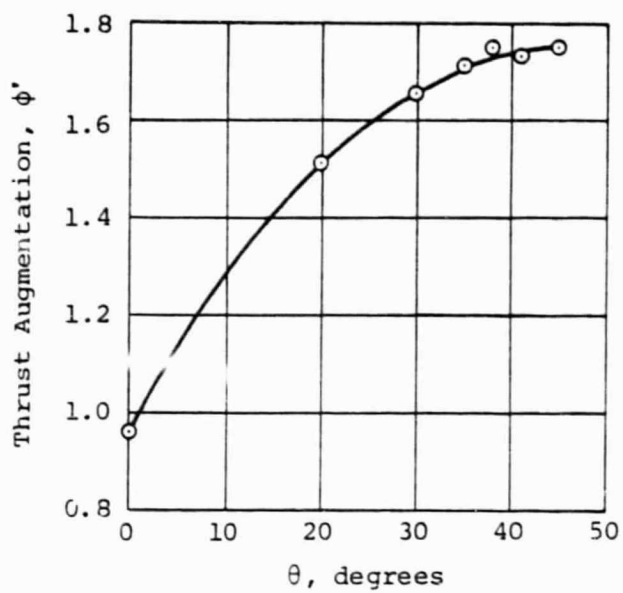


Figure 4 Adjustable, Tubular Nozzles, Adjacent to Inlet Surface Geometry and Performance

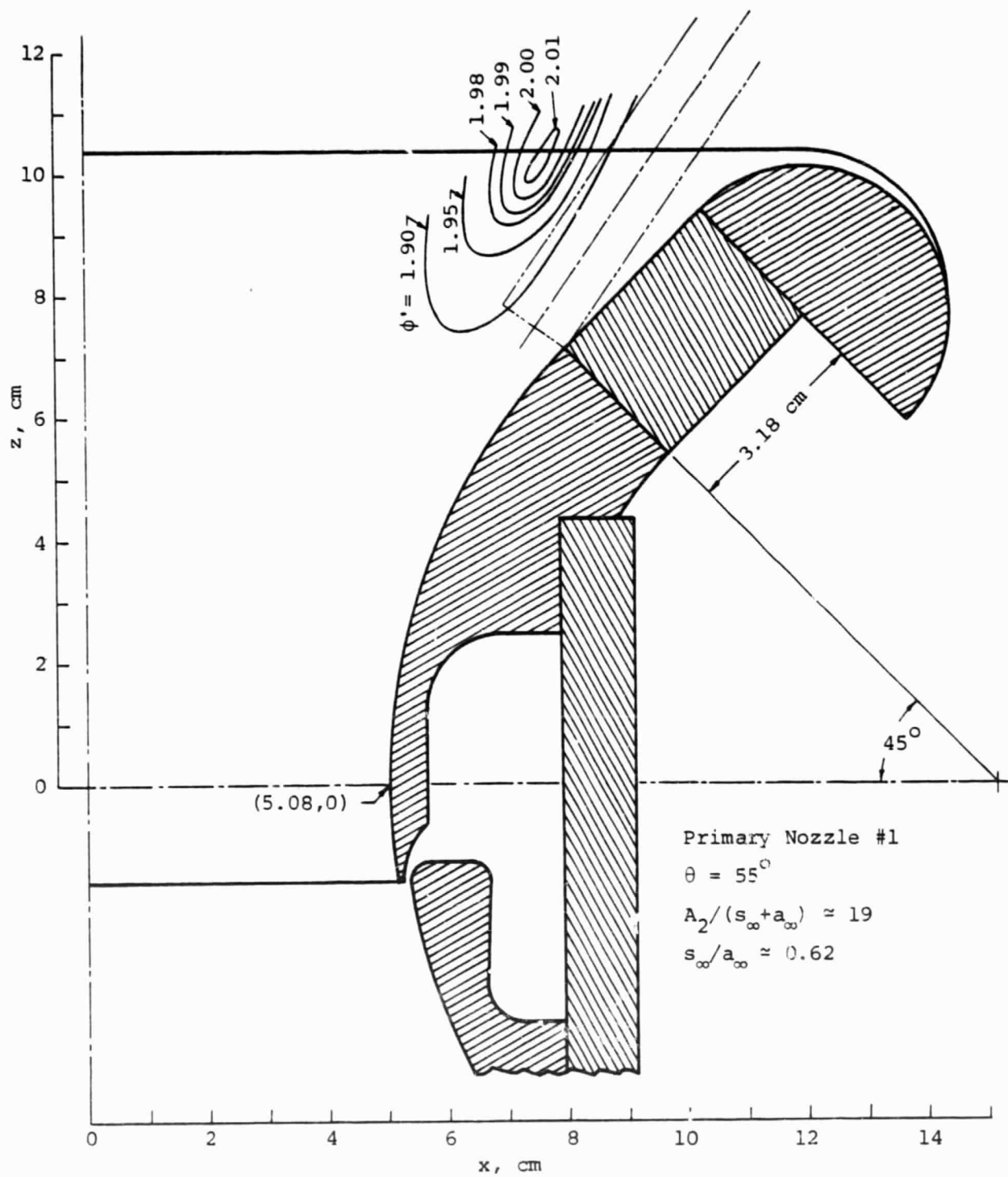


Figure 5

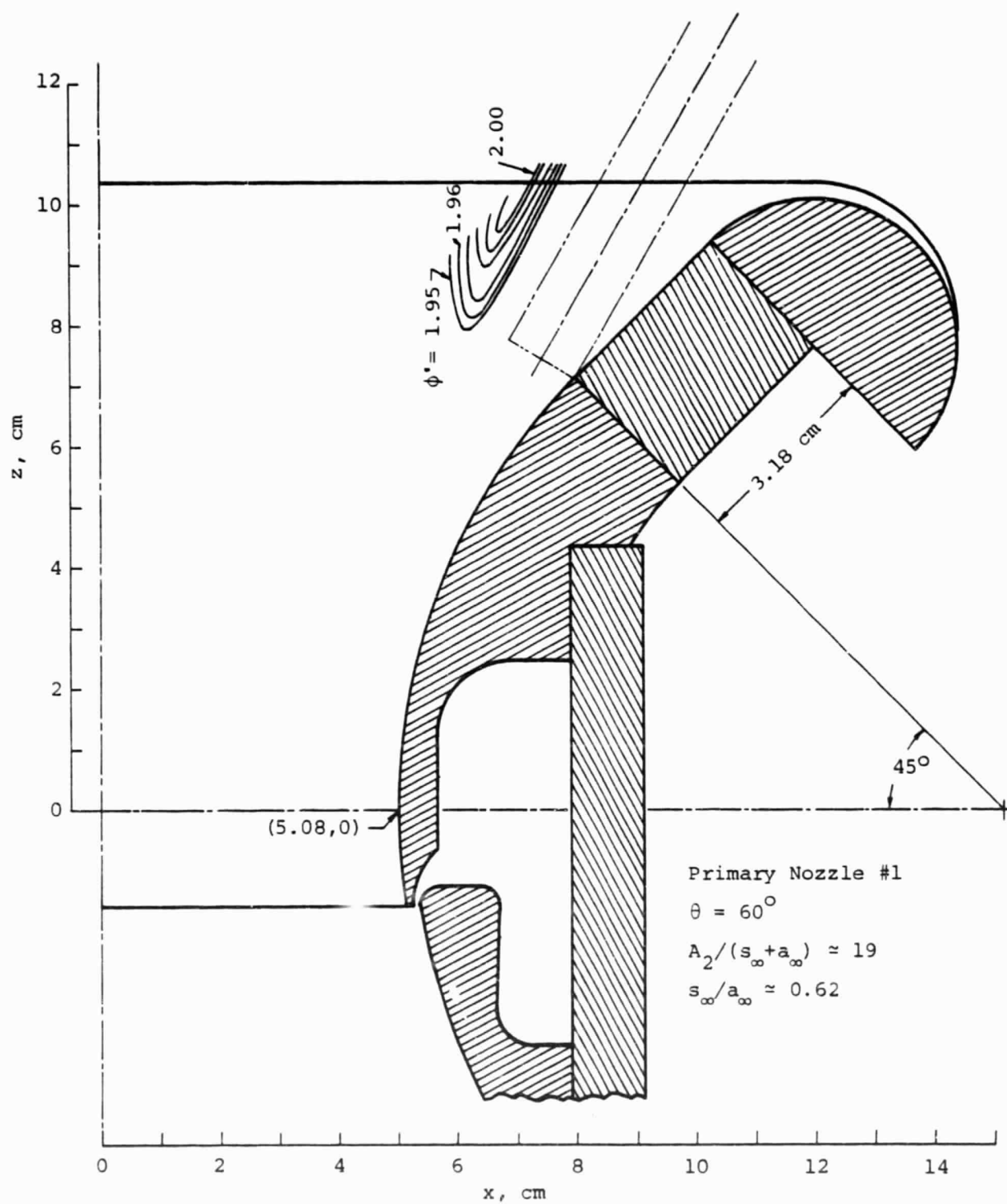


Figure 6

ORIGINAL PAGE IS  
OF POOR QUALITY



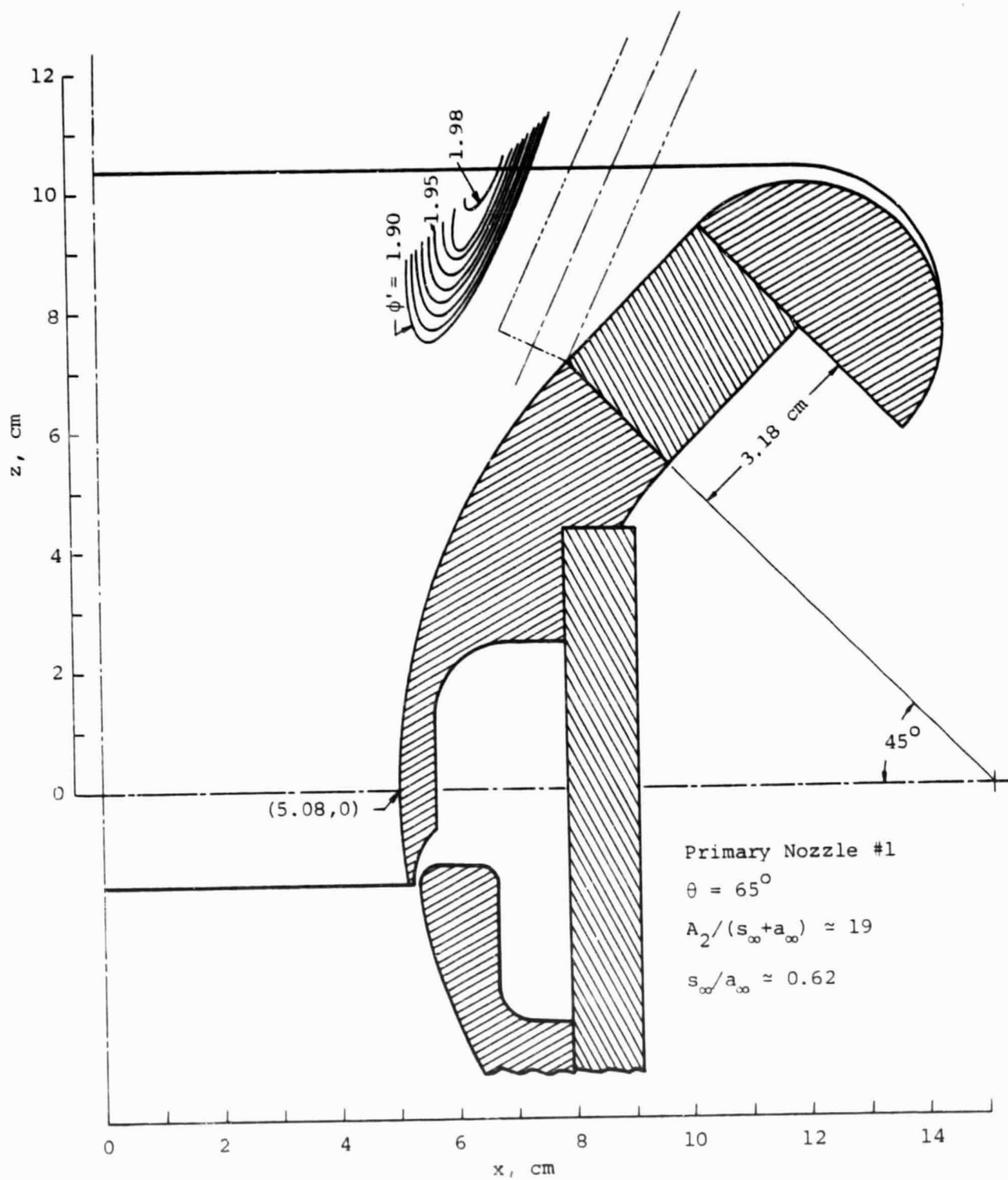


Figure 7

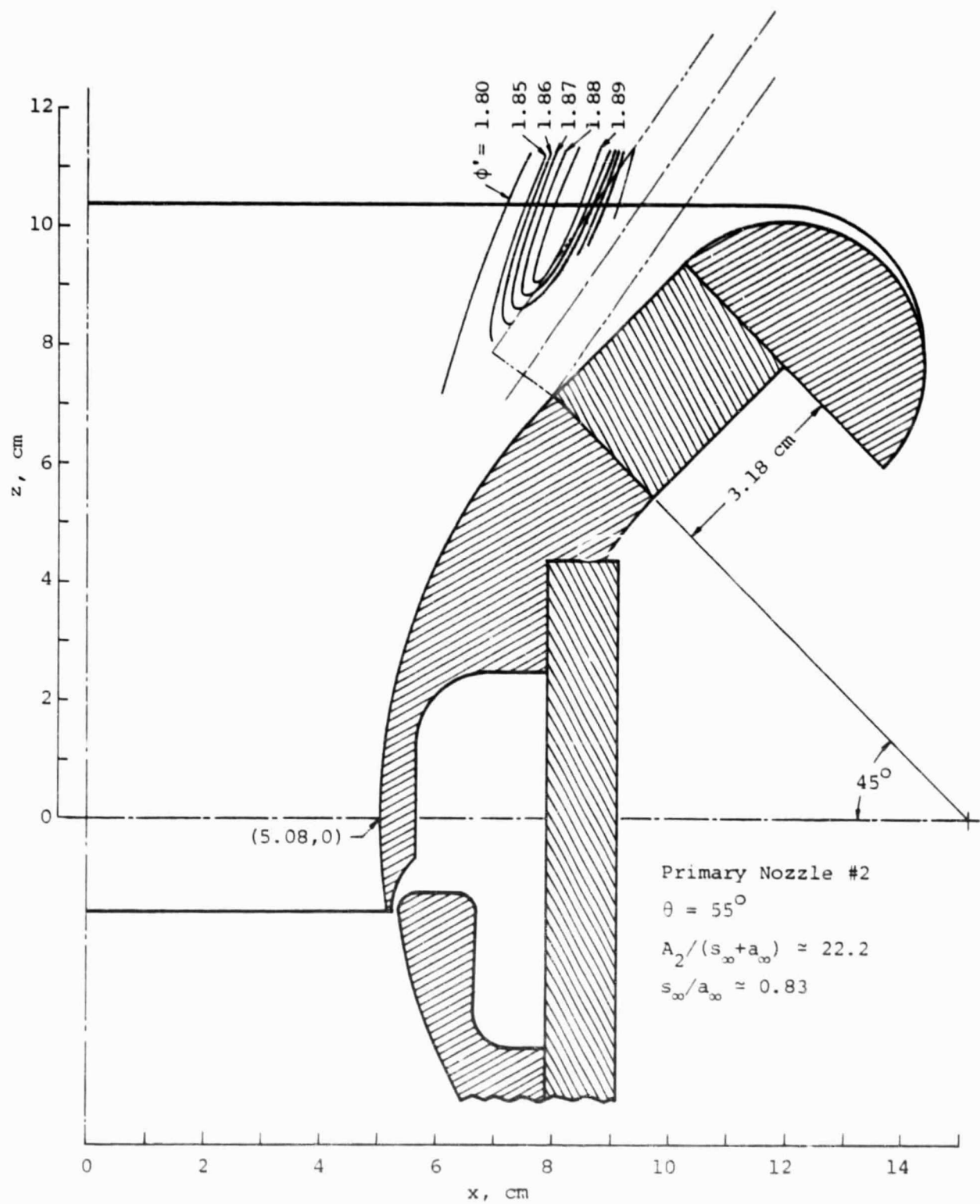


Figure 8

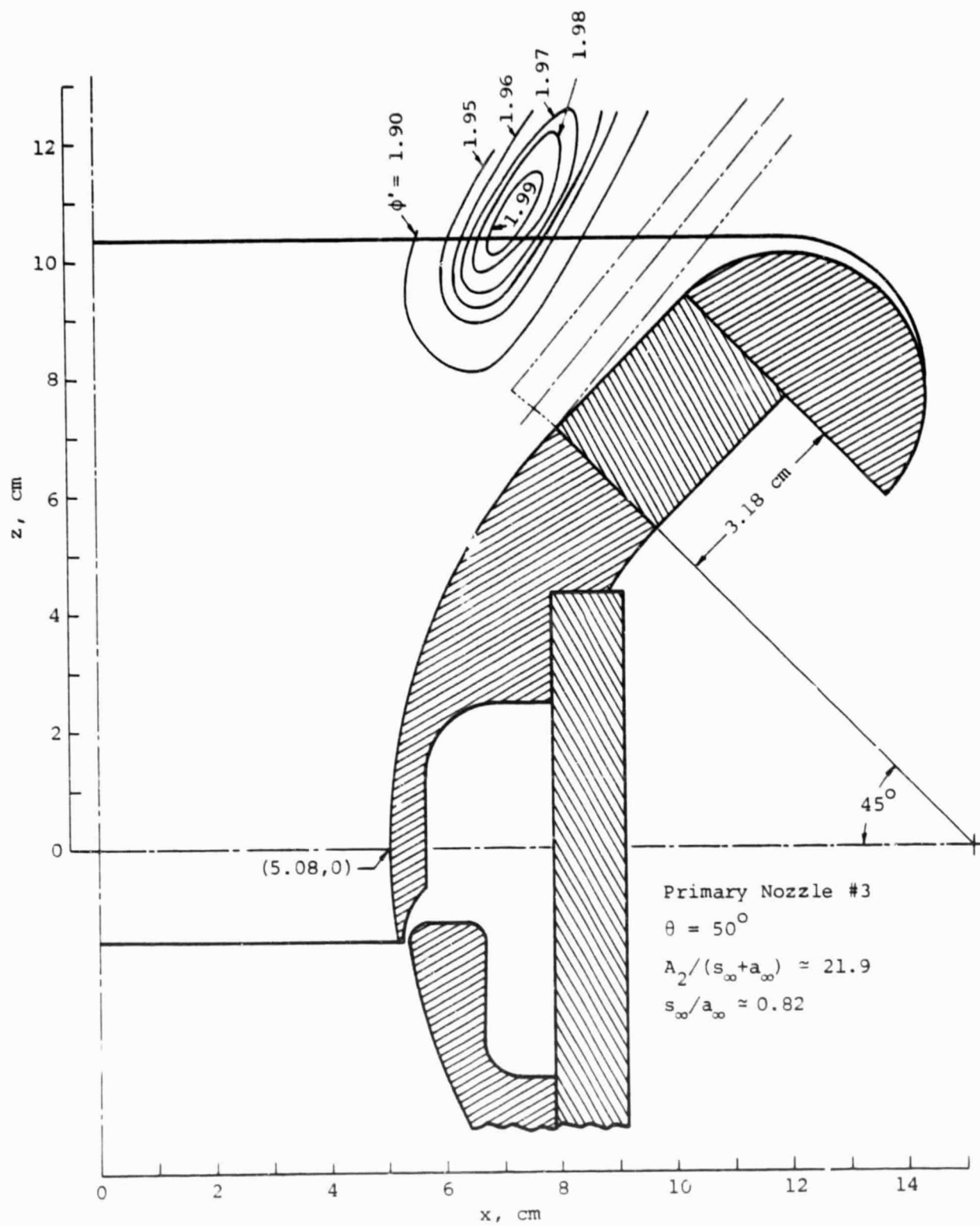


Figure 9

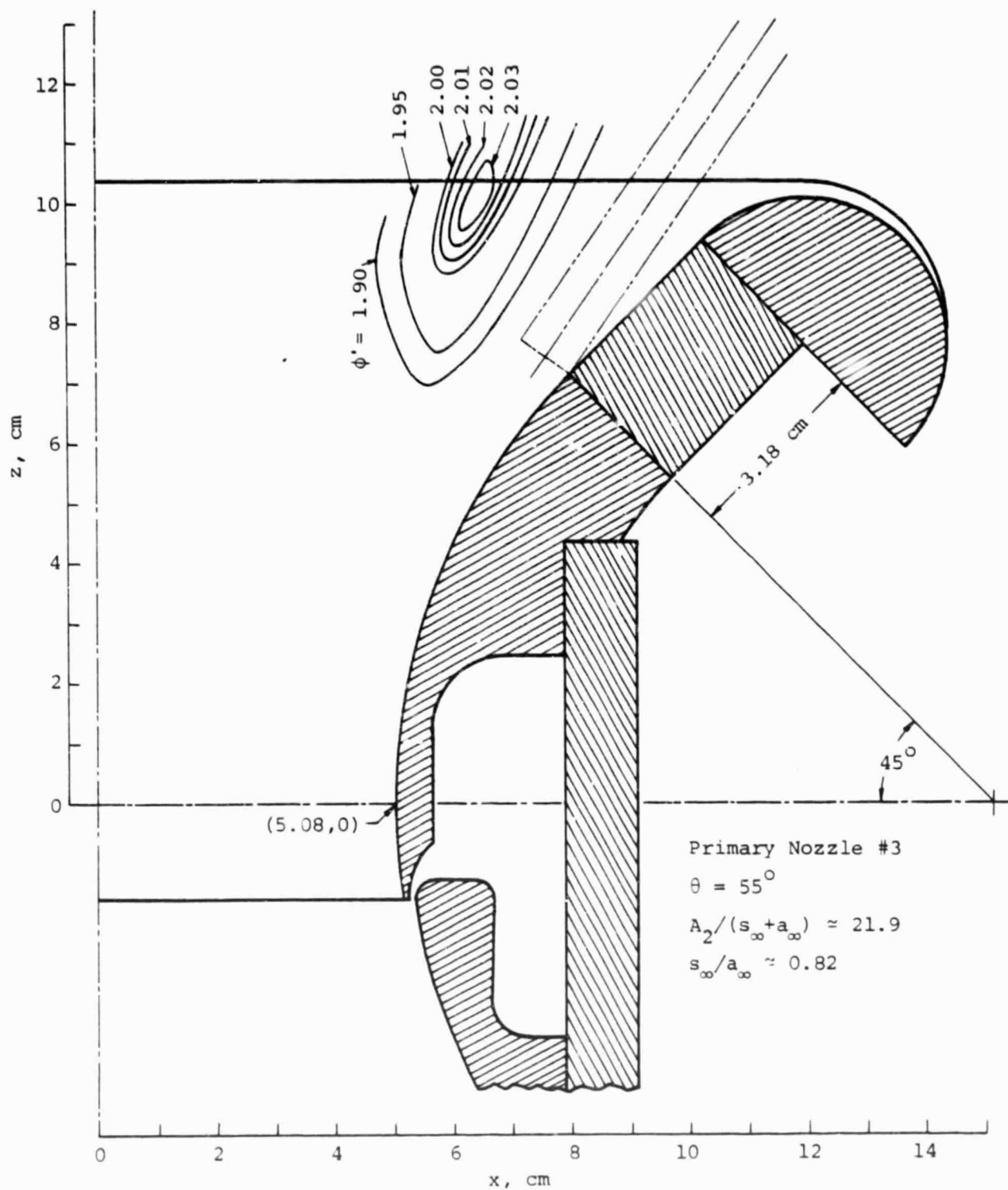


Figure 10

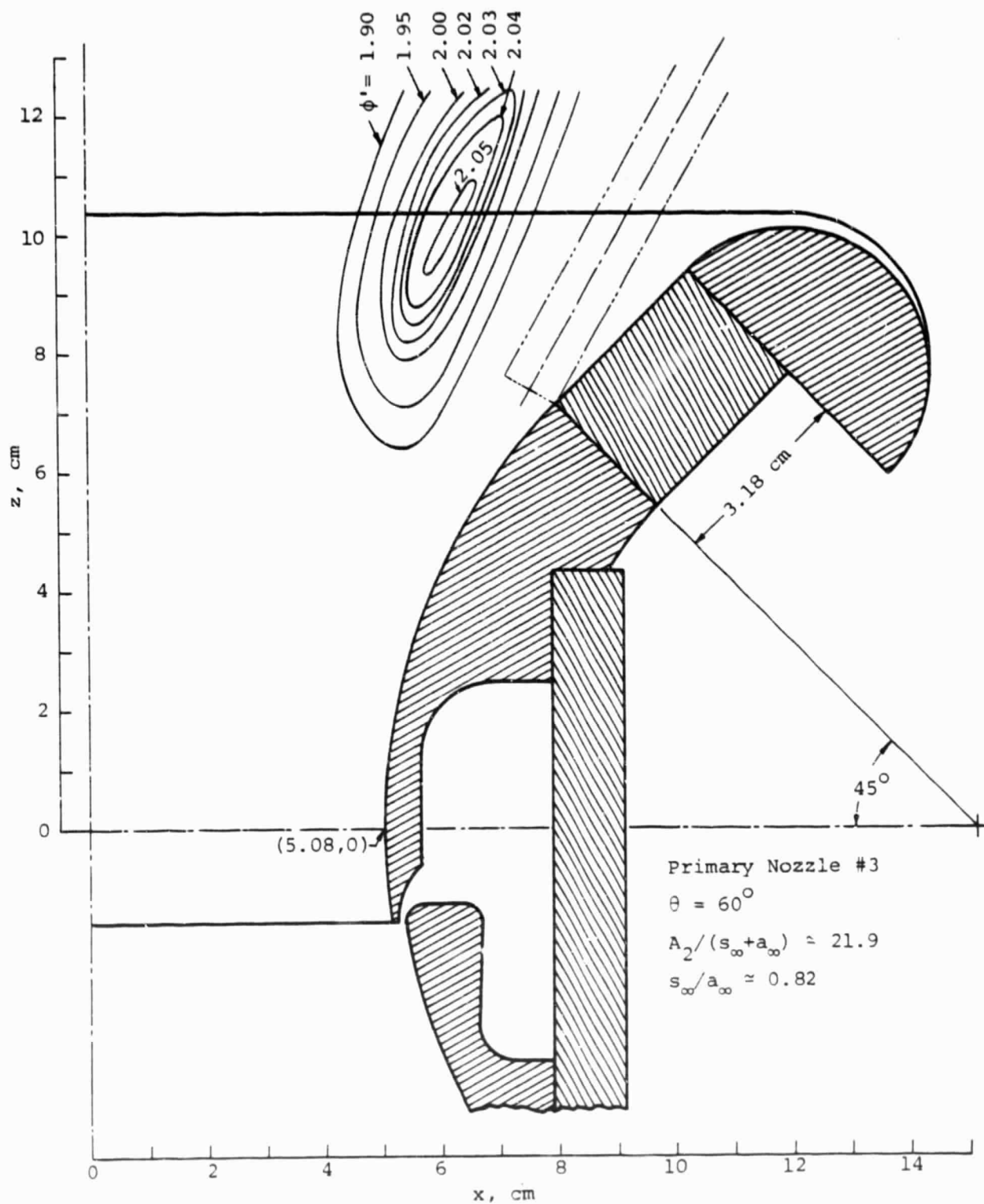
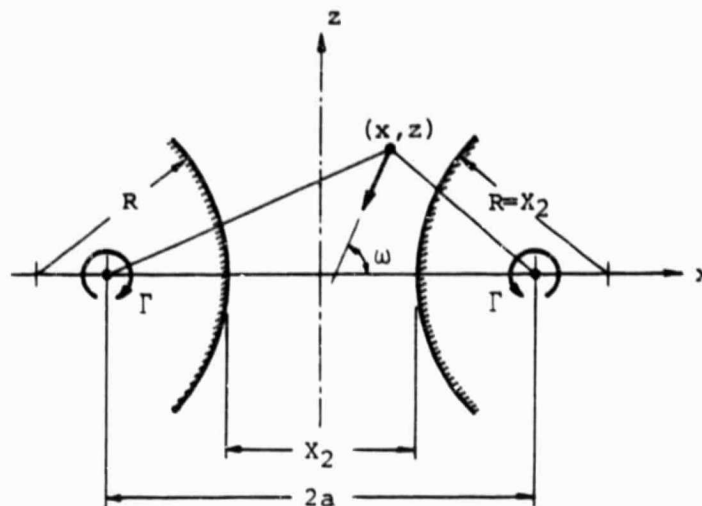


Figure 11

ORIGINAL PAGE IS  
 OF POOR QUALITY

Figure 12  
Potential Flow Model  
of Ejector Inlet



Since the ejector inlet is basically a two-dimensional design, a potential flow model can be used to correlate the experimental results. For an ejector duct which consists of two identical cylindrical surfaces separated by a distance which corresponds to their radius of curvature, as shown on Figure 12, the stream function for the flow within the duct can be described by the methods of Reference 4.

Thus, for a pair of two-dimensional, counter rotating vortices, the stream function  $\psi$  is,

$$\psi = \frac{\Gamma}{4\pi} \ln \frac{z^2 + (x - a)^2}{z^2 + (x + a)^2}$$

where

$$a = \sqrt{5/4} X_2$$

and the local flow angle ( $\omega$ ) with respect to the thrust axis is expressed as;

$$\omega = 90^\circ - \sin^{-1} \left[ \left( \frac{z}{a} \right) \frac{1 - \exp (4\pi\psi/\Gamma)}{1 + \exp (4\pi\psi/\Gamma)} \right]$$

It is shown in Reference 2 that the experimentally measured pressure distribution is very closely similar to that given by the above method.

A summary of the test results of the adjustable tubular nozzles, at their approximate position of best performance (Fig's 5 through 11), and theoretical correlation of the induced flow derived from the two-dimensional potential flow is presented in Table I.

Table I  
Adjustable Primary Nozzles

Primary Nozzle				Max. Performance (Experiment)				Induced Flow	
No.	Spacing cm	I.D. cm	O.D. cm	$\theta$ deg	$\phi'$	x cm	z cm	$1 - \frac{\psi}{\psi_w}$	$\omega$ deg
1	3.81	0.940	1.270	55	2.01	7.6	10.4	0.30	57.7
				60	2.00	7.1	10.2	0.33	59.4
				65	1.98	6.6	10.2	0.37	61.0
2	6.35	1.092	1.270	55	1.89	8.4	10.7	0.27	55.2
3	2.54	0.704	0.953	50	1.99	7.4	10.9	0.35	57.9
				55	2.03	6.4	10.2	0.39	61.7
				60	2.05	6.4	10.2	0.39	61.7

It is important to point out that:

1.  $(1 - \psi/\psi_w)$  is a measure of the amount of induced flow between the nozzle exit plane and the inlet surface, compared to the overall induced flow (since  $\psi = 0$  at the center line ( $x=0$ ), the unsubscripted  $\psi$  refers to the stream function at the plane of the nozzles and the subscript "w" is used to designate the stream function at the wall, or inlet surface). To achieve optimal performance, this quantity is about one-third.

2.  $\omega$  is the angle of the induced flow (derived from theory) defined with respect to the normal to the thrust axis (Fig. 12). The best ejector performance occurs when  $\omega$  is very close to  $\theta$ . This means that attempts to accelerate mixing by creating vorticity of large strength (crossing primary and induced flow at large angles) may not be desirable.

As indicated in Table I, Nozzles 1 and 3 produced the largest thrust augmentations. The relatively low performance of Nozzle No. 2 is attributed to its large spacing between nozzles and the large area of each individual jet, which may result in an inadequate mixing for this nozzle orientation.

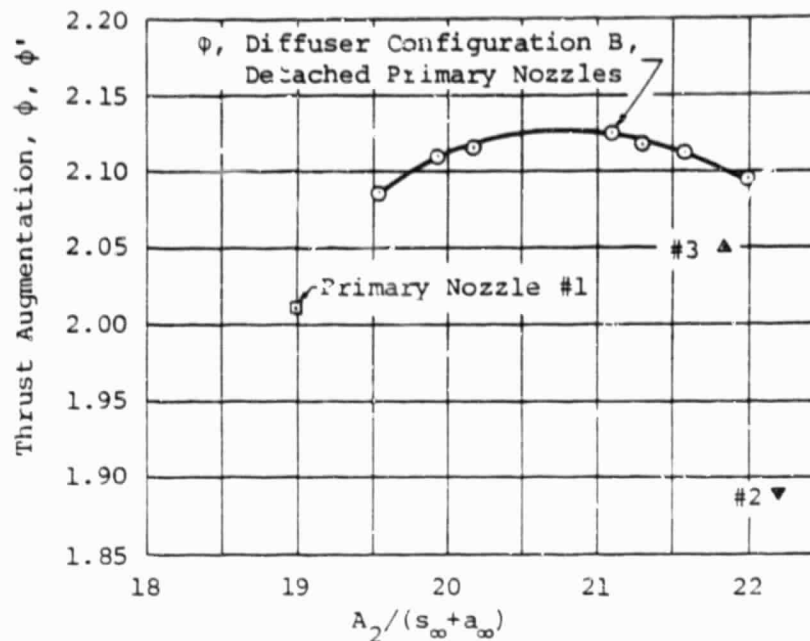


Figure 13 Performance of Jet-Diffuser Ejector With Adjustable Nozzles, Compared to Performance with Detached Nozzles

Although in designing these adjustable nozzles, an attempt was made to select the most suitable inlet area ratio ( $A_2/(s_\infty + a_\infty)$ ), for the Configuration B diffuser, the use of standard tubing sizes precluded exact duplication of this characteristic. The result of this design consideration is shown plotted on Figure 13, where typical inlet area ratios achieved with each set of nozzles is shown plotted vs the maximum thrust augmentation achieved by each, and comparison is made with the data acquired with detached nozzles (Reference 2).

Comparative evaluation of the above data, and consideration of:

1. suitability for integration into a V/STOL ejector wing,
2. minimal performance penalty during ejector operation due to;
  - a. location, orientation and spacing,
  - b. internal and external losses,

resulted in the selection of Nozzle No. 3 at an exit coordinate of ( $x = 5.59$  cm and  $z = 8.44$  cm) with a  $60^\circ$  orientation and a corresponding  $\phi' = 2.03$  as a design choice.



### Attached Nozzles

Since the adjustable tubular nozzle optimization study was performed with simple circular tube nozzles, the design of the attached nozzles required consideration of the internal and external shapes to avoid excessive losses. Initially, a set of attached nozzles (designated No. 4) was designed to discharge the primary fluid as prescribed by the adjustable tubular nozzle study. The internal duct of these nozzles was of a continuously reducing cross-section, elongated at the root while turning to a 60 degree inclination with a circular exit, as illustrated on Figure 14. The external fairing consisted of a NACA 0023 Airfoil at the root chord (in the flow direction) where the flow direction is known to be inclined in the direction of the ejector inlet surface. The chord of the fairing decreased towards the tip as is also illustrated on Figure 14. The combined effects of a decreasing chord, a fixed thickness and a change of the flow direction towards the axis of symmetry of the ejector, resulted in an estimated nozzle tip thickness/chord ratio of 35%.

Testing of the No. 4 nozzles indicated a high internal flow efficiency, but exhibited an instability in the external (induced) flow, due to separation from the external fairing surfaces of the nozzles, precluding steady state force measurement. To alleviate this instability, the chord length of the nozzle fairing was increased (No. 4A) as illustrated on Figure 14 in dashed lines.

The ejector with primary nozzles having extended fairing chords (No. 4A), eliminated the instability observed with the No. 4 nozzles, and provided a measured thrust augmentation of 2.02 at an area ratio  $A_2/(s_\infty + a_\infty) = 21$ . As can be observed on Figure 13, this performance was somewhat less than that of the same ejector with detached STAMP primary nozzles. The ejector performance penalty was attributed to the increased blockage of the inlet, a slight increase of internal loss as will be shown in Table III, and perhaps less complete mixing, resulting from the use of the attached nozzles. The maximum attached nozzle fairing thickness of the No. 4A primary nozzles was 1.067 cm, which represents a blockage of 42%, since the nozzles are spaced at 2.54 cm.

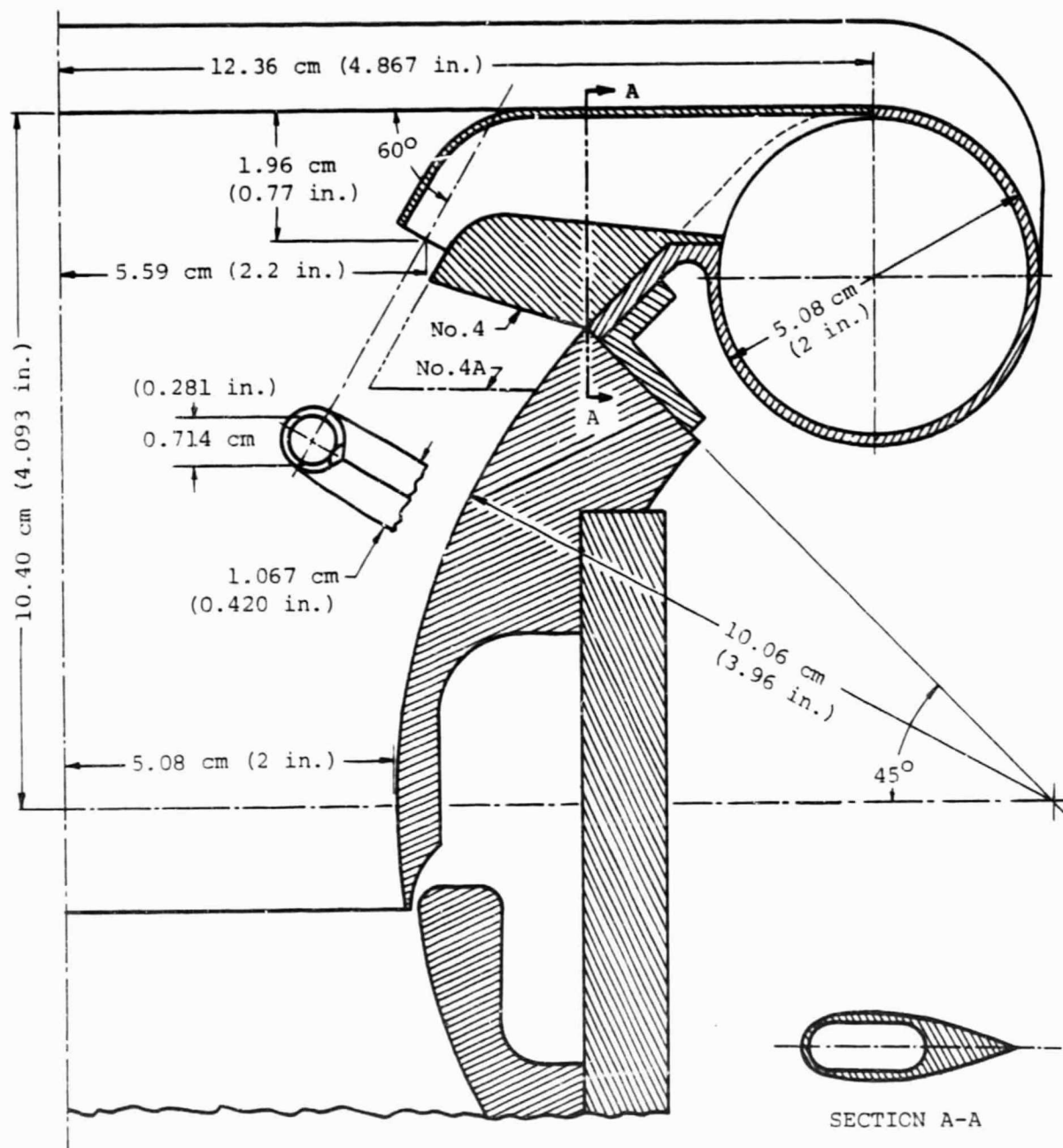


Figure 14 Attached Primary Nozzles No. 4 and 4A  
Mounted on Jet-Diffuser Ejector

The large blockage of this attached nozzle design resulted in several undesirable effects including:

1. increased loss in the induced flow
2. shifting of the best location of the nozzle exit, compared to that determined by the adjustable tubular nozzle study
3. sensitivity to large inlet disturbances.

Since stable ejector flow is essential for practical aircraft applications, the nozzles were redesigned with a reduced fairing thickness.

#### Primary Nozzle Design No. 5

This nozzle design achieved a smaller thickness and thickness ratio than that of the No. 4 and 4A designs by a reduction of the internal duct width near the root of the nozzle. To compensate for the reduced duct area due to this narrowing, the duct was elongated in the chordwise direction to avoid excessive internal duct losses. In this design (No. 5) the nozzle tip remained circular with the same area as those of the No. 4 and 4A designs in order to achieve the area ratio  $A_2/(s_\infty + a_\infty)$  close to 21, which was optimal for the current diffuser jet set-up.

The design configuration of Nozzle No. 5 and its appearance installed on the ejector are illustrated on Figure 15. Its basic dimensions and measured ejector performance, in comparison to those of the No's. 4 and 4A nozzles are summarized in Table II.

Table II  
Attached Nozzle Properties

Nozzle	Maximum Thickness t, cm	Maximum Chord* c, cm	Typical t/c Thrust Direction	t/c @ Root Flow Direction	Thrust Augmentation $\phi$
4	1.067	3.284	0.325	0.230	-----
4A	1.067	4.191	0.255	0.180	2.02
5	0.721	3.284	0.220	0.156	2.02

\* Chord is measured in the thrust direction

The blockage reduction achieved by Nozzle No. 5 design, compared to Nozzle 4A significantly improved the ejector flow stability, but the improvement of ejector performance was off-set by losses of internal flow as can be observed in the nozzle efficiency experiments described in the following section.

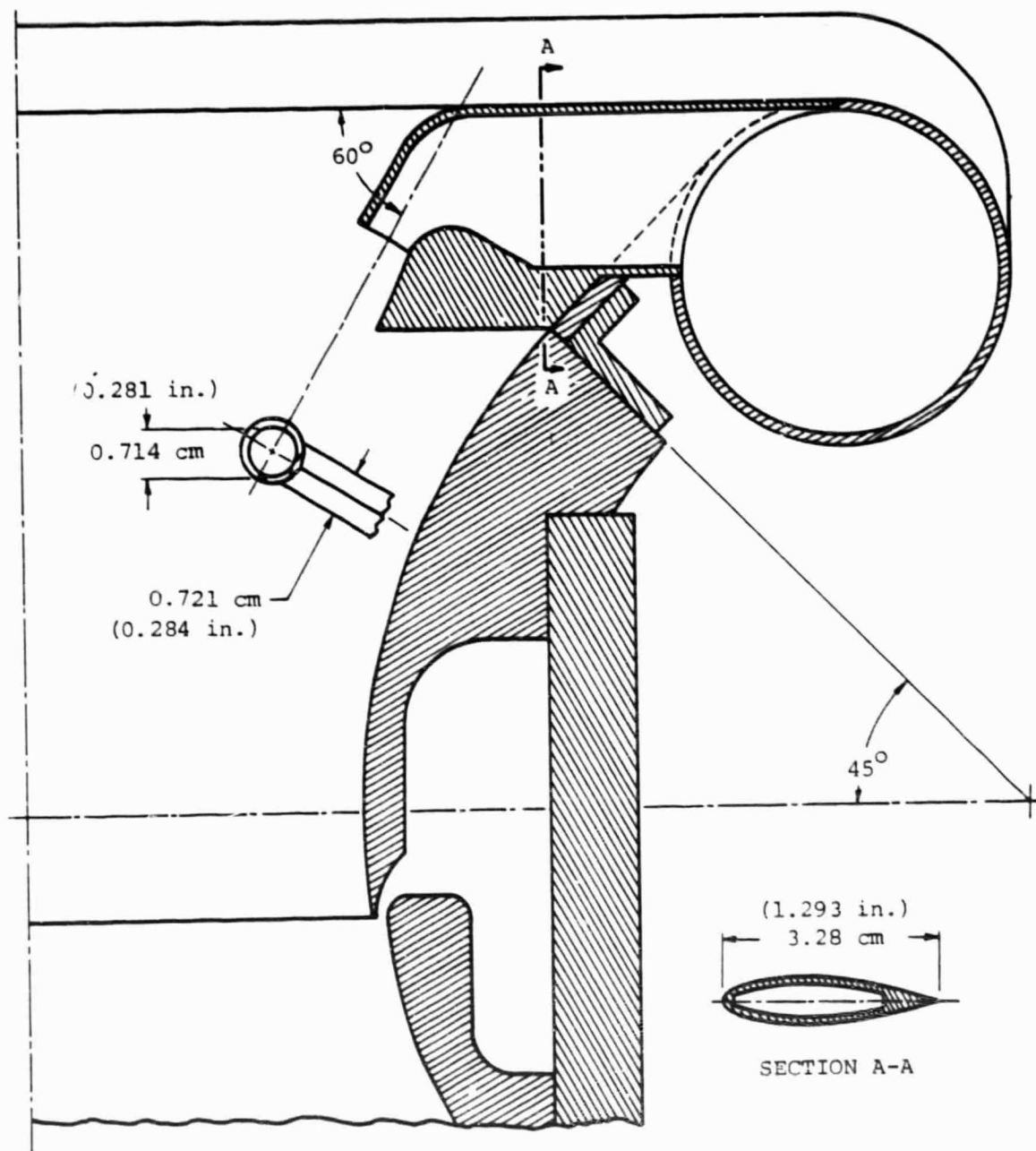


Figure 15 Primary Nozzle No. 5 on AJDE

### Primary Nozzle Performance

By mounting the detached nozzles (shown in Fig. 1) and nozzles 4A and 5 on the static test rig without the ejector, (to avoid the influence of the local flowfield in the actual ejector installation) measurements of the plenum conditions, mass flow and thrust of each set of nozzles, permitted evaluation of the discharge coefficient and the thrust efficiency.

#### Discharge Coefficient

The discharge coefficient (C) is defined as the ratio of the measured mass flow to the mass flow resulting from isentropic expansion from the plenum pressure to ambient pressure through the measured nozzle exit area (A). Thus

$$\dot{m}_{\text{isentropic}} = p_{\infty} A \sqrt{\frac{2}{n R T_{\text{op}}}} (P_{\text{op}}/P_{\infty})^n \left[ (P_{\text{op}}/P_{\infty})^n - 1 \right]$$

and

$$C = \dot{m}_{\text{measured}} / \dot{m}_{\text{isentropic}}$$

The discharge coefficient determined in this manner is presented in Table III.

#### Thrust Efficiency

The thrust efficiency ( $\eta_N$ ) is defined as the ratio of the measured thrust to the thrust resulting from an isentropic expansion of the measured mass flow from the plenum pressure to ambient pressure, thus

$$\eta_N = F_{\text{measured}} / \dot{m}_{\text{measured}} V_{\text{isentropic}}$$

where

$$V_{\text{isentropic}} = \sqrt{(2/n) R T_{\text{op}} \left[ 1 - (p_{\infty}/P_{\text{op}})^n \right]}$$

The thrust efficiency determined in this manner is presented in Table III.

Table III  
Nozzle Performance

Primary Nozzle	Discharge Coefficient	Thrust Efficiency
Detached STAMP	0.93	1.00
4A	0.88	0.98
5	0.84	0.96

The larger loss (smaller thrust efficiency) of the No. 5 nozzle compared to the No. 4A nozzle is attributable to the more elongated internal duct and smaller turning radius.

As indicated in Figure 13, the STAMP ejector with its original, detached primary nozzles achieved a thrust augmentation of 2.13. However, the similar ejector configuration with attached nozzles achieved a thrust augmentation of 2.02. The improved integrability (into a high speed aircraft) of the ejector with attached nozzles compensates for the performance penalty. However, it is of interest to note that the performance penalty associated with the attached nozzle design is attributable to several aspects of the design, some of which may be evidenced only under the test conditions utilized in this study, while others are intrinsic to the change of location of the nozzles.

For example, the attached nozzles, being located in a region of relatively high speed, compared to the location of the detached STAMP nozzles, would produce a larger drag or loss of momentum in the induced flow. Attempts to minimize this external loss by minimization of the blockage area and skin friction, as previously described, contribute to the increased internal nozzle loss.

The internal nozzle losses are comprised of skin friction and turning loss, both of which are Reynolds No. dependent. Nozzle Design No. 5 has a smaller turning radius and the more elongated duct than that of No. 4 or 4A, thereby incurring a greater turning loss. At the test conditions of 24.1 kilopascals (3.5 psig), and assuming ideal exit flow velocity and actual diameter, the Reynolds No. of the internal flow is about  $9 \times 10^4$ . This Reynolds No. is known to be in the region of very large turning loss and increases of the Reynolds No. resulting from operation at higher pressures, or larger size, will reduce this loss, as indicated in Section I, Part A, of Reference 5. Therefore the No. 5 nozzle design is considered superior to that of the No. 4A nozzle design, in view of the improvement in flow stability and the expected equivalence of thrust efficiency at higher Reynolds No. operation.

## SENSITIVITY STUDY

Integration of V/STOL ejectors into aircraft configurations are frequently accompanied by surface irregularities and leaks due to the requirement for hinges and/or tracks associated with the stowage or closure of the ejector opening during conventional flight. Evaluation of the influence of these irregularities on the ejector performance is necessary in order to provide design information for avoidance of serious performance degradation.

The jet-diffuser ejector with attached nozzle Design No. 5 was modified by superposition of surface protrusions, depressions and plenum leakage at the most probable locations for occurrences of these irregularities as a result of design requirements or operational damage, as suggested by the Navy. A summary of the locations of the surface irregularities tested is presented on Table IV and illustrated schematically on Figure 16.

Table IV  
Surface Irregularities

	Inlet	Throat	Diffuser
Center of Span	Protrusion	Protrusion	Protrusion
	Plenum leak	Plenum leak	
	Asymmetry		
Corner and end	Protrusion	Protrusion	Protrusion
	Plenum leak	Plenum leak	
	Depression		

Dimensions, locations and influence on performance of these surface irregularities are described in the following text.



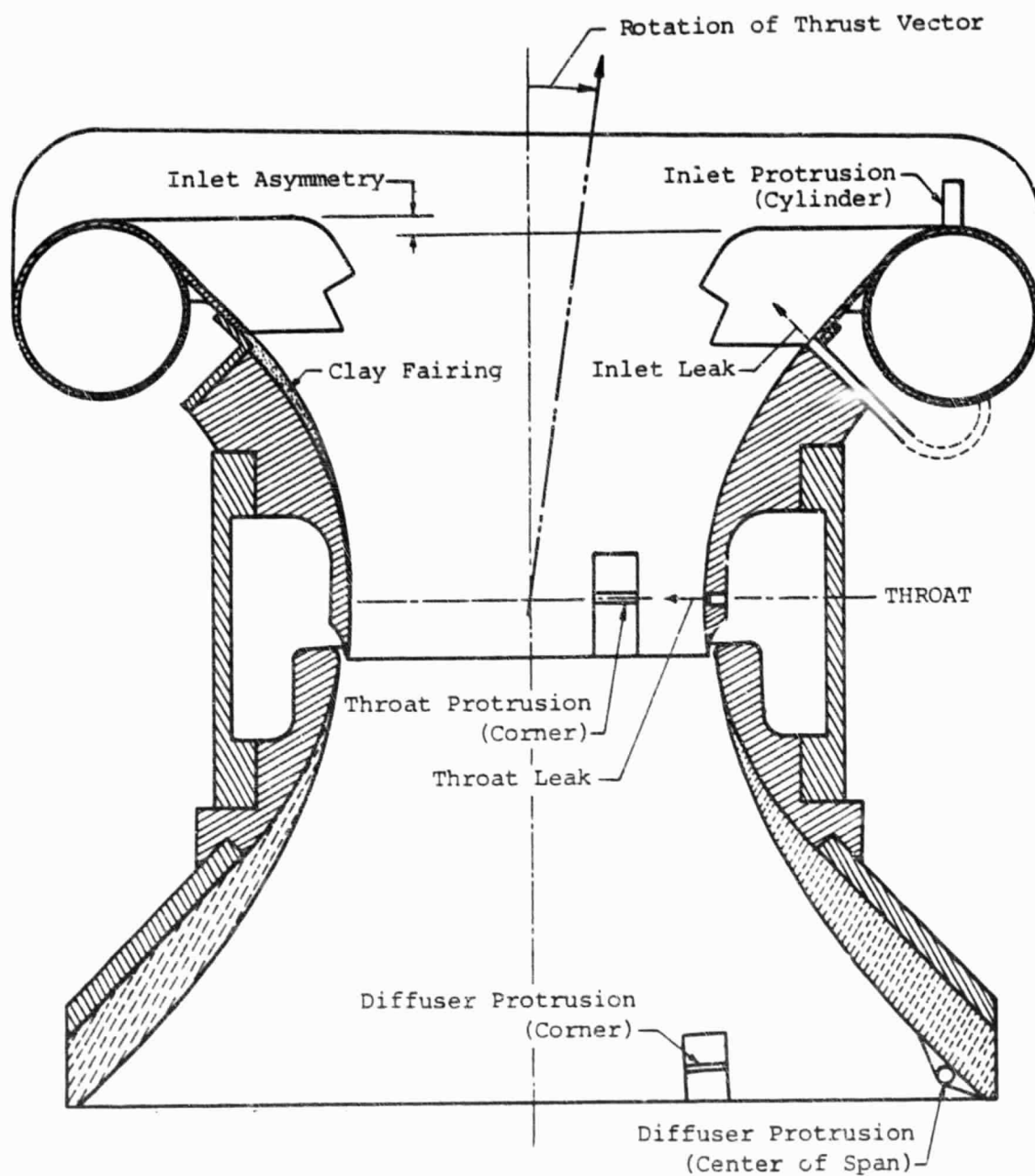


Figure 16 Jet-Diffuser Ejector - Cross-Section  
with Surface Irregularities



The surface irregularities consist of three sets of protrusions (cylindrical rods), depressions, leaks and asymmetries. Dimensions of the protrusions are presented in Table V.

Table V  
Dimensions of Surface Protrusions

Size	Diameter cm (in)	Length cm (in)
1	0.114 (0.045)	0.318 (0.125)
2	0.229 (0.090)	0.635 (0.250)
3	0.457 (0.180)	1.270 (0.500)

Physical descriptions of protrusions, depressions, leak arrangements and asymmetries are discussed in the text along with their influence on ejector performance in terms of  $\Delta\phi$ , the change in thrust augmentation due to the presence of the irregularities.

#### Inlet Surface Irregularities

##### Protrusions

##### Corners

Four Size 3 protrusions were attached to the top of the inlet lip, between the end walls and the closest primary nozzle, one at each of the four corners. No measurable effect was produced by the largest size protrusion and therefore the smaller sizes were not tested.

##### Center of Span

Two Size 3 protrusions were attached to the top of the inlet lip, at the center of the span one on each side of the ejector. No measurable effect was produced by the largest size protrusions and therefore the smaller sizes were not tested.

## Plenum Leakage

### Corner

A leak orifice of 0.079 cm (0.031 in) diameter was drilled on a surface plate with thickness of 0.051 cm (0.020 in) at one corner and connected to a tube with inside diameter of 0.185 cm (0.073 in) leading from the primary plenum to the surface plate. The leak was located between the end wall and the nearest nozzle, its center is about 0.159 cm (0.063 in) above the 45° inlet joint of the ejector. The leak improved ejector performance by an increase of thrust augmentation of +0.01. No rotation of the thrust vector was detected.

### Center of Span

A leak orifice of 0.079 cm (0.031 in) diameter was drilled on a surface plate with thickness of 0.051 cm (0.020 in) at the center of the span on one side of the ejector and connected to a tube with inside diameter of 0.185 cm (0.073 in) leading from the primary plenum to the surface plate, near the 45° line (Fig. 16). This leak produced an increase of thrust augmentation of +0.02 and no detectable rotation of the thrust vector, as compared to the undisturbed ejector.

Plenum leakage near the inlet of the ejector improved performance. This appears to be the result of improvement of mixing and injection of leak flows with a higher nozzle efficiency than that of the primary nozzles. The small leakage contribution to performance improvement can probably happen only when the flow field is well established by the existence of the primary and the diffuser jet flows. The improvement is a good indication that the primary nozzle design can be further improved.

## Depression

### Corner

A depression having the dimensions of 1.27 cm (0.5 in) long, 0.23 cm (0.09 in) deep and 0.23 cm (0.09 in) wide was milled into the end inlet block near one corner of the ejector. No measurable effect on the performance was observed.

### Asymmetry

One entire side of the inlet was moved upstream, protruding 0.653 cm (0.25 in) further upstream than the opposite side of the ejector, and resulting gaps and irregularities were filled with clay, as illustrated previously on Figure 16. As a result of this asymmetry, the thrust vector was rotated by 1 degree away from the disturbed side of the ejector and the augmentation was not affected.

### Throat Irregularities

#### Protrusions

##### Corner

Protrusions were attached on the end walls of the ejector, at the throat, with centers about 2.54 cm (1.0 in) from the plane of symmetry. With one Size 2 protuberance, no measurable effect on the thrust augmentation was observed. However, with Size 3 a decrease in thrust augmentation of about 0.01 was observed. No rotation of the thrust vector was observed.

##### Center of Span

All three sizes of protrusions were installed at the throat, (about 1.63 cm (0.64 in) upstream of the diffuser jet slot), at the center of the span of the ejector. Each size was attached and faired with a flat clay surface about 3 diameters forward and aft of the protrusion, similar to the diffuser protrusions illustrated on Figure 16. The influence of each protrusion on the thrust augmentation is described in Table VI below.

Table VI  
Influence of Throat Protrusions  
at Center of Span

Size	$\Delta\phi$	Rotation of Thrust Vector*	Remarks
1	None	None	
2	-0.01	3 deg	No Flow Separation
3	-0.20	13 deg	Flow Separation

\* towards the disturbed side

Protrusions appear to have significant influence on performance only when flow separation occurs.

## Throat Irregularities (Cont'd)

### Plenum Leakage

#### Corner

A leak orifice of 0.079 cm (0.031 in) was drilled at the corner, 45 degrees from the end and side walls, and 1.63 cm (0.64 in) upstream of the diffuser jet slot. This orifice was connected to the plenum similarly to the plenum leak at the center of the span shown on Figure 16. At the corner, the influence on performance was not measurable.

#### Center of Span

A leak orifice of 0.079 cm (0.031 in) was drilled into the throat of the ejector at a position 1.63 cm (0.64 in) upstream of the diffuser jet slot. The orifice was connected to the plenum as illustrated on Figure 16. This leak resulted in a rotation of the thrust vector by 1/2 degree towards the disturbed side of the ejector. No measurable change in the thrust augmentation was observed.

## Diffuser Irregularities

### Protrusions

#### Corner

A Size 3 protrusion was installed at 1.27 cm (0.5 in) upstream of the diffuser exit, on the end wall 5 cm (2 in) from the plane of symmetry of the ejector. The protruding rods were faired with flat surfaces about 3 diameters forward and aft of the protrusion, as illustrated on Figure 16.

The largest protrusion did not influence the ejector performance, and therefore smaller protrusions were not tested.

#### Center of Span

One Size 3 protrusion was installed in the center of the span of the ejector, about 1.27 cm (0.5 in) upstream of the diffuser exit. The protruding rod was faired in a manner similar to the protrusion near the corner, as shown on Figure 16.

The largest size protrusion produced a rotation of the thrust vector of 1/2 degree towards the disturbed side with no measurable effect on thrust augmentation. Therefore the smaller sizes of protrusions were not tested.

## CONCLUSIONS

1. Primary nozzles which do not protrude from the body of a jet-diffuser ejector can be designed to provide equivalent performance to that of the ejector with detached, protruding nozzles, thus providing an extremely compact ejector.
2. Coanda turning, which represents a method for minimization of the inlet drag, results in large performance degradation due to frictional loss of the primary fluid if turning is rapid and due to opposing jet impingement if turning is less rapid. The net result at optimal turning provides lower performance than that with detached nozzles or properly designed attached nozzles.
3. The performance of the ejector is strongly dependent upon the location and orientation of the point of injection of the primary fluid.
4. The design of non-protruding, attached primary nozzles requires careful consideration of the minimization of internal turning losses and external fairing shapes which must avoid separation and must minimize blockage of the induced flow.
5. Primary Nozzle No. 4A has a better internal flow performance than that of Nozzle No. 5 at the Reynolds Number of the present test condition. But Primary Nozzle No. 5 has a better performance than that of No. 4A in the external (induced) flow. For most ejector applications, the Reynolds No. of the primary nozzle flow is expected to be higher than that of the present experiment, and the ejector performance penalty due to internal flow loss of the primary nozzle is expected to decrease. Therefore the more compact design of Primary Nozzle No. 5 is preferred to that of 4A.
6. The throat region of the ejector, where local ejector flow velocities are a maximum is the most sensitive region to surface irregularities. The fact that a small plenum leak near the inlet improves the ejector performance, indicates that further investigation of this phenomenon may lead to an improvement of primary nozzle design.

#### REFERENCES

1. Alperin, M., Wu, J.J. and Smith, C.A. "The Alperin Jet-Diffuser Ejector (AJDE) Development, Testing, and Performance Verification Report", Flight Dynamics Research Corp., Naval Weapons Center, NWC TP 5853, February 1976
2. Alperin, M., Wu, J.J. "End wall and Corner Flow Improvements of the Rectangular Alperin Jet-Diffuser Ejector", Flight Dynamics Research Corp., Naval Air Development Center, NADC-77050-30, May 1978
3. Spink, L.K. "Flow Meter Engineering", The Foxboro Co. Ninth Edition 1967
4. Prandtl, L. and Tietjens, "Fundamentals of Hydro and Aeromechanics", Dover Publications, Inc. New York, N.Y. 1934
5. "Aero-Space Applied Thermodynamics Manual", SAE, Inc. Jan. 1962